Direct Evidence of Torque-mediated Optical Magnetism

M. Tuan Trinh[1*], Krishnandu Makhal[1], Elizabeth F.C. Dreyer[1], Apoorv Shanker[2], Seong-Jun Yoon[2], Jinsang Kim[2], and Stephen C. Rand[1,3]

Magnetic properties of materials that can be controlled with applied electric fields or light enable novel sensing technology, energy conversion, ultrafast data storage, and non-reciprocal photonic technology [1-8]. Hence the topic of magnetoelectric phenomena which provide a means of coupling electric and magnetic effects in bulk media has attracted widespread interest [9]. However no mechanism has been demonstrated to support or enhance intense magnetism in systems free of spin-orbit or spin-spin interactions at the molecular level. In this paper energy-resolved spectra of scattered light, recorded at moderate intensities (10^8 W/cm^2) and short timescales (<150 fs) in a series of non-magnetic molecular liquids, reveal the signature of a unique optical nonlinearity driven jointly by the electric and magnetic field components of light that accomplishes this. Radiant magnetization is reported at the optical frequency through a magneto-electric interaction at the molecular level, and stimulated librational features are shown for the first time to appear uniquely in the spectrum of cross-polarized scattering. These findings confirm that magnetic torque actively mediates the enhancement of induced magnetism and accounts for the parity-time (P-T) symmetry of this new class of nonlinearity, in excellent agreement with quantum theoretical predictions.

In bulk material, the coupling of magnetic and electric processes generally takes place through intermediate fields. That is, magneto-electric interactions are mediated by magnetostriction and piezoelectricity. For example, the application of a magnetic field in a low symmetry magnetic material causes magnetostriction which in turn causes an electric field to appear via the piezoelectric effect [5]. In this way a coupling is established between electric and magnetic effects, allowing magnetic energy to be converted to electric energy or vice versa. Given the availability of magnetic materials with couplings to electric phenomena, there is considerable interest in combining electronic and magnetic properties to create multifunctional devices based on magneto-electric and multiferroic materials. At the present time however such devices rely on magneto-electric properties of bulk solids [9] or magnetic thin films [6], making them difficult to miniaturize. There is no apparent way to extend their operation to the nanoscale. While magneto-electric interactions at the nanoscale or molecular level have been discussed in the literature [10-12], and have recently been observed [13], no mechanism for them has ever been confirmed. In particular, no evidence of specific dynamics attributable to the optical magnetic field has been presented to date. Moreover the conventional wisdom in nonlinear optics is typically invoked to dismiss effects of the optical magnetic field, owing to the smallness of the Lorentz driving force that it produces (which is proportional to $B=E/c$, where c is the speed of light). This is perfectly justified unless an enhancement mechanism were to exist to magnify the Lorentz force of light. Hence it is important to determine whether the fundamental mechanism that has been theorized to enhance optical magnetism driven by the combined optical fields E and H at the level of individual molecules [14] is correct. We present the first direct experimental evidence that torque by the optical magnetic field, which is theoretically capable of enhancing radiant magnetization at optical frequencies, does indeed accompany magneto-electric interactions at the molecular level.

[1]Dept. of Electrical Engineering, University of Michigan, Ann Arbor, MI 48109-2099
[2]Dept. of Materials Science, University of Michigan, Ann Arbor, MI 48109
[3]Dept. of Physics, University of Michigan, Ann Arbor, MI 48109
* Correspondence and requests for materials should be addressed to M.T.T. (email: tuantrin@umich.edu)

Ultrafast magnetic response was studied in pulsed optical experiments using a simple 90° scattering geometry (Figure 1(a)). Despite the extensive literature on depolarized light scattering [15-21], there have been few reports of the complete radiation patterns which are necessary to distinguish between electric dipole (ED) and magnetic dipole (MD) or higher order response at the molecular level, or to investigate the question of whether light is capable of inducing strong, radiant magnetization [13,22]. In the present work we correct this oversight. Early studies revealed that collisional effects took place in gases and liquids and generated a small amount of depolarization even in isotropic molecules at low light intensities, on long timescales (exceeding the collisional reorientation time). However no experiments were performed at high enough intensities or sufficiently short timescales to discriminate between collisional depolarization and magnetization on the basis of the angular distribution of scattered radiation or by performing suitable spectral analysis. Here we utilize moderately high intensities ($I \sim 10^8 W/cm^2$) and ultrashort pulses ($\tau_p < 150\ fs$) to record both the radiation patterns and the spectrum of scattered light. Our experimental results disclose key details of the mechanism governing radiant optical magnetization in dielectric media for the first time.

The magnitude of an induced magnetic dipole moment m is normally limited to a small fraction of the electric dipole p, namely $m/p < \alpha$, where $\alpha = 1/137$ is the fine structure constant. Exceptions occur in media where spin-spin interactions are strong or the ED approximation is not upheld, such as in ferromagnets, structured dielectrics, metamaterials, and nanoparticles. However strong magnetic response is not expected in natural homogeneous (non-magnetic) materials at high frequencies. For this very reason, highly engineered, non-uniform materials offer an important route to realizing magnetic response via (static) structural design. In the present work, an intriguing alternative is revealed however. Dynamic nonlinear interactions offer possibilities that extend beyond structural design. In particular, optical interactions obeying parity-time (P-T) symmetry due to the optical magnetic field can cause dynamic symmetry-breaking which enables radiant magnetization [23]. This provides a route to supersede traditional limitations on the magnetic moment. In the current paper the results of our investigation of a P-T symmetric magneto-electric nonlinearity [24] are shown to confirm that magnetic optical torque can play an essential role in creating strong magnetic response in nominally non-magnetic media, by enabling an ultrafast exchange between orbital and rotational angular momentum [14, 24] which enhances the magnetic moment.

Results

The experimental setup utilized an amplified femtosecond laser system (Amplitude Inc.) operating at 800 nm and delivering pulses of 0.5 mJ at a rate of 10 kHz over an electronically-tunable bandwidth of 15 to 100 nm. The laser output was used to probe the induced magnetic response of dielectric liquids composed of tetrahedral molecules. Samples included CCl_4, $SiCl_4$, $SiBr_4$, $Si(OCH_3)_4$, and $Si(OC_2H_5)_4$. These molecules exhibit isotropic optical response at low powers and represent a series in which the moment of inertia increases systematically. Complete radiation patterns were recorded in co-polarized and cross-polarized light-scattering geometries at 90° with respect to the incident beam by rotating the input polarization angle θ through 360 degrees under computer control. A schematic of the setup and a typical set of raw data for co- and cross-polarized signals for CCl_4 are shown in Figures 1(a) and 1(b). The corresponding radiation patterns are plotted in Figure 1(c), after subtraction of the unpolarized components (constant backgrounds) shown in Figure 1(b). The dependence on input intensity of the cross-polarized scattering was

previously shown to be quadratic [13]. Radiation patterns for all samples showed the same unpolarized and dipolar components with low residuals as in CCl_4 .

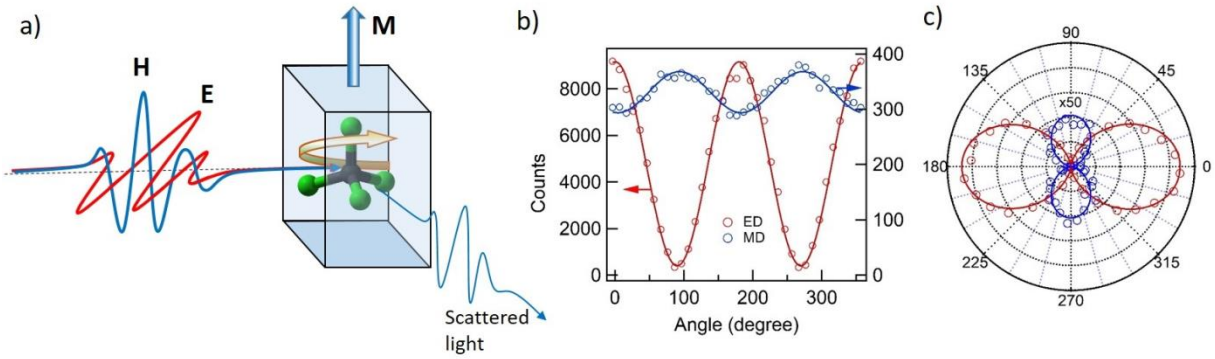

Figure 1. Schematic of the optical interaction and dipole radiation patterns from scattering experiments. (a) The optical electric field causes an electric dipole transition which imparts orbital kinetic energy to the molecule. This energy is subsequently converted to (magnetic) librational motion by the optical magnetic field. The induced electric and magnetic dipole moments cause incoherent scattering at an angle to the incident beam. (b) Raw data for co-polarized (red) and cross-polarized (blue) scattering intensities versus input rotation angle in CCl_4. (c) Radiation patterns of the co- and cross-polarized light-scattering data after subtraction of the constant (unpolarized) background evident in Fig. 1(b). The solid curves are fits to a $\cos^2\theta$ function.

A key result of this work is shown in Figure 2, which displays the normalized spectra of scattered light recorded with a 0.5 m grating spectrometer for co-polarized and cross-polarized signals. The co-polarized (Rayleigh scattering) spectrum in red is virtually indistinguishable from the instrumental response over the bandwidth reflecting the pulse duration (See Supporting Information (SI)). The cross-polarized spectrum in blue has large additional features in it which may be emphasized by subtracting the co-polarized signal to obtain the difference spectrum shown in grey. The extra features appearing in the cross-polarized spectrum are then seen to correspond to inelastic scattering from known rotations and vibrations of CCl_4. Below the grey curve the expected positions and relative heights of rotationally- and vibrationally-shifted satellite lines are indicated by vertical bars. Co- and cross-polarized spectra for the other samples are shown in Figure 3 (a)-(c). Experimental values of the rotation and vibration energies were determined by convolving the instrumental response $I(\omega)$ with an assumed spectrum of satellite lines of variable height and position and proceeding to make a multivariate fit to the data. The results for fitted vibration and rotation frequencies are in good agreement with literature values (see SI). The comparison of experimental rotation frequencies with results from prior spectroscopy shown in Figure 3(d) provides compelling evidence for the rotational assignments and confirms the generation of rotations (librations) during the interaction responsible for cross-polarized scattering.

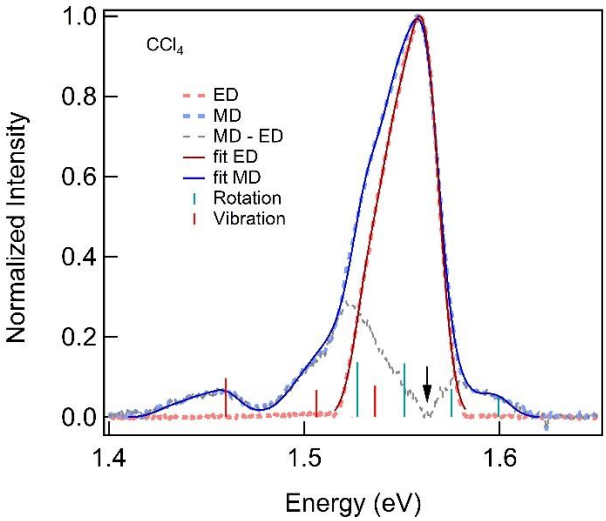

Figure 2. Normalized co- and cross-polarized scattered light spectra in CCl_4. The red curve is the Rayleigh signal (labelled ED), which peaks at the black arrow. The blue curve is the cross-polarized signal (labelled MD), with the solid curve showing a best fit that takes instrumental linewidth into account together with inelastic components due to vibrational and rotational transitions as indicated by vertical red and blue bars. The grey curve is the difference between the red and blue curves, highlighting the inelastic components in the MD spectrum.

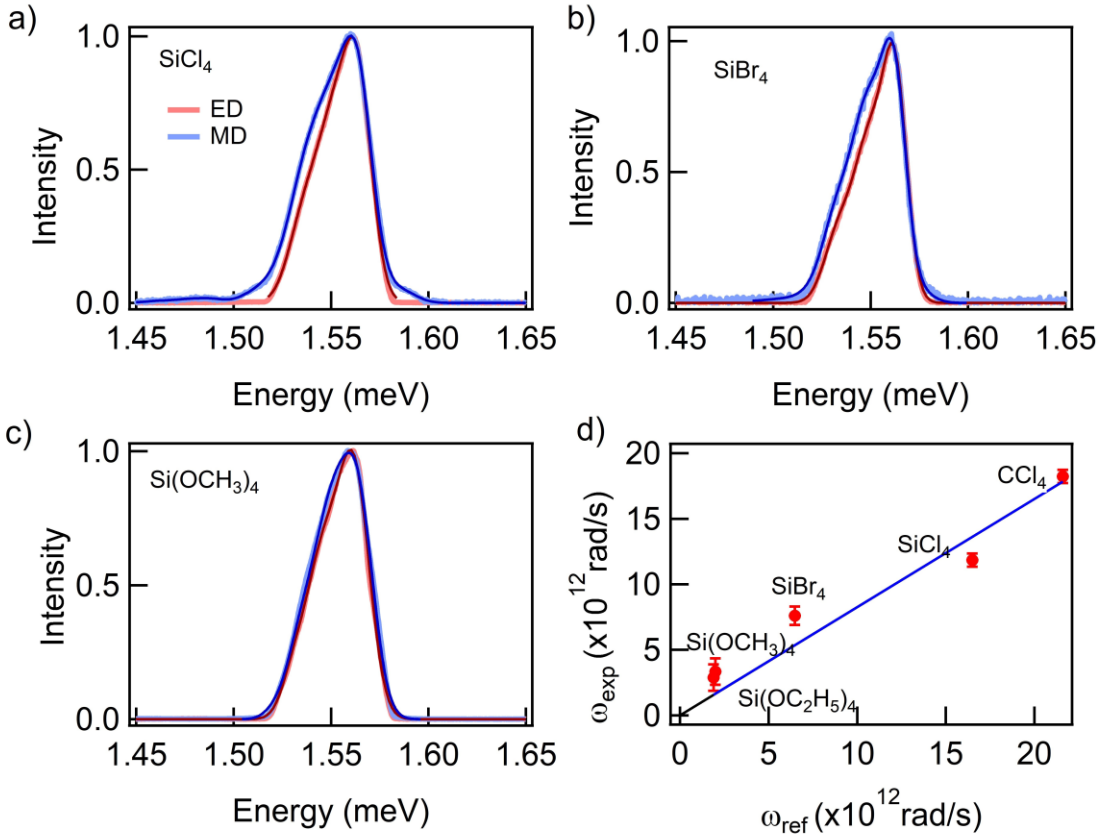

Figure 3. Normalized co- and cross-polarized scattered light spectra (labelled ED and MD respectively) for various compounds. (a) $SiCl_4$, (b) $SiBr_4$ and c) $Si(OCH_3)_4$ with fitted

curves. (d) The experimental rotation frequencies ($\omega_{\exp}$) plotted versus literature values (ω_{ref}) for all samples [25,26]. The solid line is a linear fit with a slope of 0.85.

The result of analyzing the polarization states of inelastic scattered light components is shown in Figure 4. This measurement was made by recording complete spectra at discrete values of θ separated by steps of 30° and determined whether particular spectral features were polarized, unpolarized or of mixed polarization. In the plot, the elastic component at the center of the cross-polarized (MD) spectrum dropped substantially as the input field was rotated away from horizontal (90°). This indicated that it was composed of a dipolar contribution to the scattered light with a large unpolarized background. Spectral features at large shifts (1.4 to 1.53 eV) on the other hand did not vary at all as the input polarization was varied. Hence these features were completely unpolarized. In the next section we discuss the close correspondence of these findings with expectations from the quantum theory of magneto-electric interactions at the molecular level.

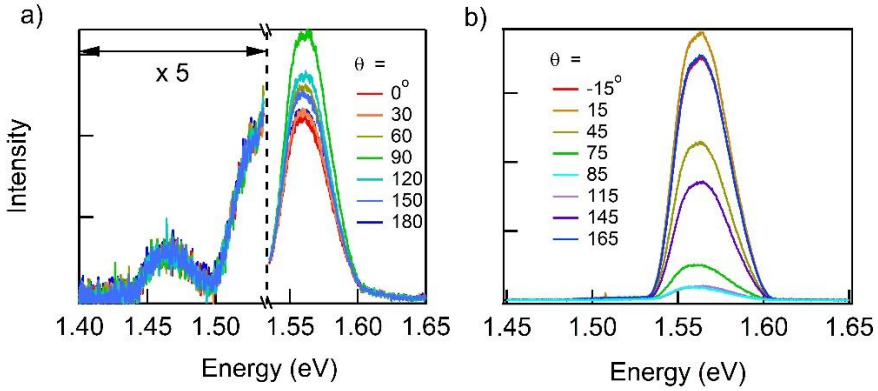

Figure 4. Polarization dependence of cross-polarized (a) and co-polarized (b) spectra in CCl_4. θ is the pump polarization angle. In (a) the window from 1.40 to 1.53 eV has been magnified 5 times for clarity to show there is no polarization dependence. The input angle θ=0° corresponds to vertical polarization. In (b) the entire spectrum is highly polarized.

Discussion

Many physical processes cause depolarization in light scattering. The term itself refers to either loss of polarization or the generation of components orthogonal to the input fields. Hence it may originate from collisionally-induced rotations, collisional dipole-dipole interactions, electric torque acting on anisotropic electric polarization (in the case of anisotropic molecules), electric torque acting on Kerr-induced anisotropy in isotropic molecules, or magneto-electric interactions at the molecular level. Of these various processes, only dipole-dipole collisions, Kerr effects and magneto-electric interactions can occur on timescales faster than the molecular re-orientation time. (The timescale of magneto-electric interactions is calculated explicitly at the end of this discussion). So these are the only candidates for explaining cross-polarized components in light scattering. However dipole-dipole interactions and Kerr effects do not yield radiation patterns similar to those measured experimentally. Colliding molecules could instantaneously produce a depolarized probe field E_{probe} resulting for example in an optical Kerr polarization [27] of the form $P_z=\varepsilon_0\chi_{zzxx}(E_{probe})_z E_x E_x$, but the angle-averaged probe field would be zero since it is randomly oriented. Hence this mechanism does not add significantly to the radiation pattern at all. At sufficiently high intensities, a Kerr effect of the form $P_x=\varepsilon_0\chi_{xxxx}(E_{probe})_x E_x E_x$ based on a polarized probe field would contribute importantly to co-polarized light scattering. However, the three fields

that drive the nonlinearity would each contribute an angular projection to the radiation pattern. Hence the angular dependence of co-polarized light scattering would vary as $I(\theta)\sim\cos^6\theta$, resulting in a pattern which is not observed in the data of Figure 1. Hence in isotropic media such as liquid CCl_4 only the magneto-electric mechanism can produce depolarized light on femtosecond timescales with either the dipolar or unpolarized component patterns displayed in Figure 1, at the intensities of our experiments.

A magneto-electric interaction at the molecular level has been theorized [14] to proceed as shown in Figure 5. The process relies on first establishing an electric polarization in the system with the optical *E* field and in a second step converting the orbital angular momentum of the excited state to rotational angular momentum through a torque interaction driven by *H*. Two magnetic transitions are indicated by downward red arrows in Figure 5(a), corresponding to frequency components of the incident pulse that are either at the carrier frequency or at a frequency shifted down by the molecular rotation frequency ω_ϕ. The former transition is detuned from the magnetic transition by ω_ϕ and is therefore expected to be polarization-preserving. The latter transition stimulates a rotational excitation resonantly and should yield unpolarized, Stokes-shifted scattering. These two predictions are in excellent agreement with the results in Figures 2 and 4 where the extra spectral features and their polarizations are displayed. Similarly the radiation patterns of Figure 1 are in complete accord with a magneto-electric interaction at the molecular level as described above.

We note that the direct stimulation of depolarizing rotations by the resonant magnetic transition in Fig. 5(a) must cause "knock-on" vibrational excitations too. This is consistent with the presence of Stokes-shifted vibrational features in the cross-polarized spectrum of Figure 2. Moreover, the spectral features on the anti-Stokes or high energy side of the spectrum in Figure 2 are fully consistent with a "backward" transition sequence depicted in Figure 5(b). Beginning from the thermal population in rotational state 3 at room temperature, a "backward" magneto-electric transition would annihilate a rotational quantum. This yields an anti-Stokes rotational line but at the same time removes the rotational excitation necessary to cause "knock-on" vibrations during anti-Stokes scattering. Indeed no anti-Stokes features of vibrational origin are observed in Figure 2. A similar "backward" transition takes place from the second rotational energy level at room temperature but has been omitted from Figure 5(b) for simplicity. This transition accounts for the second anti-Stokes feature in Figure 2.

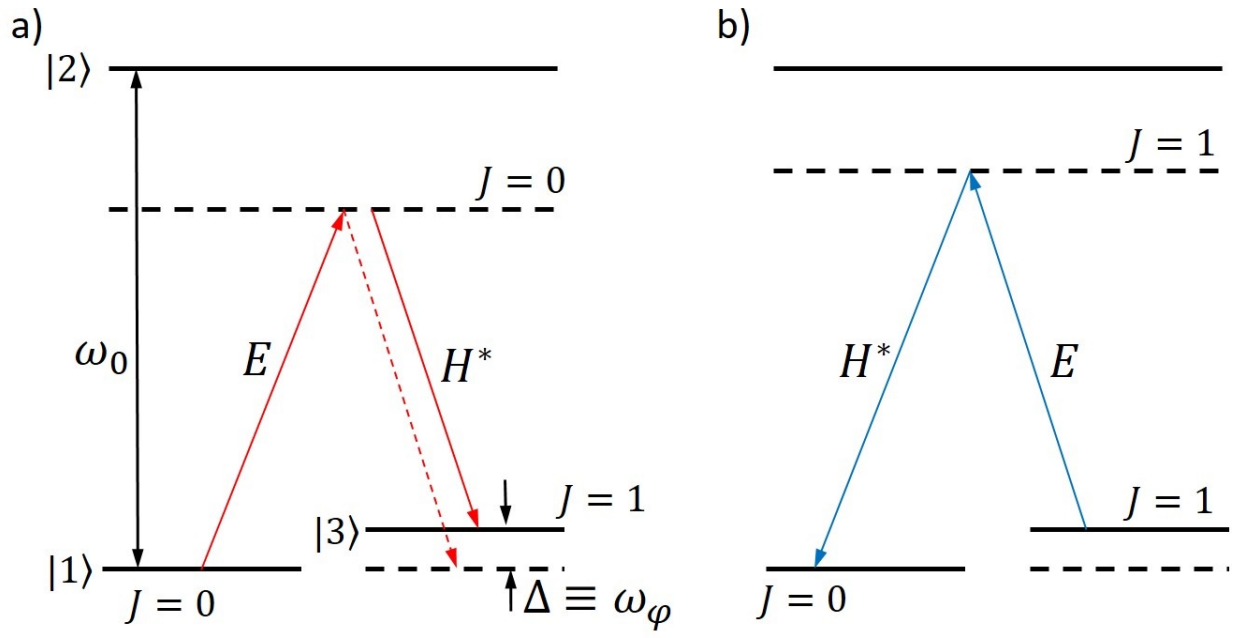

Figure 5. Two-photon transitions responsible for second-order magneto-electric scattering driven by *E* and *H* fields. (a) In the "forward" process, the *H* field stimulates two classes of magnetic transition back to the ground state, as indicated by the two downward red arrows. The magnetic transition at the laser carrier frequency ω (dashed downward arrow) is non-resonant since the terminal state is rotationally-excited. The magnetic transition at frequency $\omega - \omega_\phi$ (solid downward arrow) is resonant but can only be driven by a Fourier component of the optical pulse that is down-shifted from the carrier frequency by ω_φ (Stokes scattering). The first transition is ineffective in generating molecular rotations and produces polarized scattering. The second transition stimulates molecular rotations resonantly, giving rise to unpolarized scattering and knock-on vibrations. (b) In the "backward" process the *E* field first drives an ED transition which preserves the initial rotational state (either $J = 1$ or $J = 2$ at room temperature). Then the magnetic field stimulates an anti-Stokes MD transition at frequency $\omega + \omega_\phi$ which removes the rotation, as indicated by the downward blue arrow. This generates unpolarized anti-Stokes rotational scattering without the possibility of knock-on vibrations. The model also allows for an upward MD transition at $\omega - \omega_\phi$ followed by a downward ED transition at ω, but this has been omitted for simplicity since it does not generate a new frequency component in the scattered light.

The magnetic torque interaction analyzed in Refs. 14 and 24 enables the magnetic transitions in Figure 5 to take place at the optical frequency. While torque dynamics satisfy the quantum mechanical selection rules, they must also be ultrafast in order for the magneto-electric interaction to go to completion during the short pulse durations of our experiments. One can check that this requirement is met in our experiments by turning to the quantum mechanical torque equation. In the Heisenberg picture, the expectation value of torque expressed in terms of excited state orbital angular momentum *L* is

$$\left\langle \frac{dL_z}{dt} \right\rangle = \frac{i}{\hbar} Tr\{\tilde{\rho},\ [H^{(m)}, L_z]\} \tag{1}$$

where $\tilde{\rho}$ is the slowly-varying amplitude of the density matrix. Inserting the torque Hamiltonian $H^{(m)} = (\hbar f L'_{-} O'_{+} a^{+} - h.c.)$ from Ref. 14, Eq. (1) can be evaluated for the energy level picture of Figure 5. The torque equation reduces to

$$\frac{\hbar}{\tau} = \mu_0^{(e)} E \tag{2}$$

Transition dipole moments of the tetrahalide series range from $\mu_0^{(e)} = 4.1 \times 10^{-30} C \cdot m$ for CCl_4 to $\mu_0^{(e)} = 11.3 \times 10^{-30} C \cdot m$ for $SiCl_4$ [33]. Consequently torque completion times for the various samples at an intensity of $I = 10^{10} W/cm^2$ for example (or $E = 1.94 \times 10^8 V/m$), comparable to our experimental intensities, are found to range from $\tau = 133 fs$ down to $\tau = 48 fs$. The implication is that magnetic torque can indeed cause the exchange of orbital angular momentum for rotational angular momentum on an ultrafast timescale, allowing the magneto-electric interaction to go to completion during each pulse.

All-electric nonlinear processes like the optical Kerr effect cannot explain the radiation patterns of scattered light or the Stokes and anti-Stokes rotational spectral features reported here in (isotropic) tetrahedral molecules. Similarly, electric torque mechanisms cannot cause rotations of spherical top molecules via second- or third-order electric nonlinearities. Moreover, our observations of inelastic components in the scattered light are not the result of all-electric spontaneous or stimulated Raman processes, since vibrational and rotational features are absent from the co-polarized spectrum. All the present results were obtained far below the threshold for all-electric stimulated Raman scattering.

Conclusions

The cross-polarized spectra reported here are uniquely ascribable to a magneto-electric interaction at the molecular level, mediated by optical magnetic torque. The signal polarizations, intensity dependence, radiation patterns, and spectra are all consistent with this interpretation. By estimating the torque completion time, we have also shown that torque dynamics can be ultrafast at the intensities of our experiments. The most compelling aspect of the data is the appearance of inelastic rotational features in the MD spectrum of scattered light which are absent from the ED spectrum. These features are not consistent with Kerr nonlinearity, electric torque effects on anisotropic polarizability or purely collisional interactions. On the other hand torque dynamics in magneto-electric interactions at the molecular level can account for enhancement of radiant magnetization pulse by pulse [24], stimulation of rotations/librations and the observed modifications of the cross-polarized spectrum of scattered light. Indeed our results confirm a specific role for molecular rotations in mediating magnetization at optical frequencies, as predicted by quantum theory of molecular M-E interactions in which rotation frequency governs the 2-photon detuning [14].

A peculiarity of the magnetizing nonlinearity $M \sim EH^*$ is that despite its dependence on two optical fields the frequency of the nonlinear response is at the optical frequency rather than being a static or frequency-doubled response. This too is well-explained by a quantum interaction at the molecular level. Although the 2-photon magneto-electric transition depicted in Figure 5 is driven jointly by photons at frequencies of ω and $-\omega$ whose sum is zero, a radiant magnetization $M(\omega)$ at frequency ω is formed because the electric and magnetic dipole components of the mixed

moment $M \sim EH^*$ are orthogonal quadratures of a 2-photon magneto-electric coherence between states 1 and 3. The two quadrature moments are separately observable in scattering experiments by simply rotating the analyzer between its co- and cross-polarized orientations. The measured quadrature is then the one whose driving field, either *E* or *H*, is transmitted by the analyzer and its frequency is the optical frequency in both cases since only one quadrature is measured at a time. The first quadrature corresponds to Rayleigh scattering and the second to radiant magnetization (see Figure 1(c)). It is for this reason that the radiation patterns of both the $P \sim E$ and $M \sim H^*$ quadratures or constituents of the magneto-electric nonlinearity are each well-described by a dipolar $\cos^2\theta$ intensity distribution on an unpolarized background, rather than higher order distributions.

Methods

Methods, including statements of data availability, and any associated accession codes and references, are available at:

References

1. I. Levin, J. Li, J. Slutsker, A.L. Roytburd. Design of Self-Assembled Multiferroic Nanostructures in Epitaxial Films. *Adv. Mater.* **18**, 2044 (2006).
2. J. Das, Y.Y. Song, N. Mo, P. Krivosik, C.E. Patton., Electric-Field-Tunable Low Loss Multiferroic Ferrimagnetic–Ferroelectric Heterostructures. *Adv. Mater.* **21**, 2045 (2009).
3. N. Hur, S. Park, P.A. Sharma, J.S. Ahn, S. Guha, S.W. Cheong. Electric polarization reversal and memory in a multiferroic material induced by magnetic fields. *Nature* **429**, 392 (2004).
4. S.M. Wu, S.A. Cybart, P. Yu, M.D. Rossell, J. Zhang, R. Ramesh, R.C. Dynes. Reversible electric control of exchange bias in a multiferroic field-effect device. *Nat. Mater.* **9**, 756 (2010).
5. D. Bossini, K. Konishi, S. Toyoda, T. Arima, J. Yumoto, M.K.-Gonokami. Femtosecond activation of magnetoelectricity, *Nat. Phys.* **14**, 370 (2018).
6. V.V. Pavlov, R.V. Pisarev, A. Kirilyuk and Th. Rasing. Observation of a transversal nonlinear magneto-optical effect in thin magnetic garnet films. *Phys. Rev. Lett.* **78**, 2004 (1997).
7. M. Fiebig, D. Frohlich, T. Lottermoser, V.V. Pavlov, R.V. Pisarev, and H. –J. Weber. Second harmonic generation in the centrosymmetric antiferromagnet NiO. *Phys. Rev. Lett.* **87**, 137202 (2001).
8. C.D. Stanciu, F. Hansteen, A.V. Kimel, A. Kirilyuk, A. Tsukamoto, A. Itoh, T. Rasing. All-optical magnetic recording with circularly polarized light. *Phys. Rev. Lett.* **99**, 047601 (2007).
9. M. Fiebig. Revival of the magnetoelectric effect. *J. Phys. D. Appl. Phys.* **38**, R123-R152 (2005).
10. P. Curie. Sur la symétrie dans les phénomènes physiques, symétrie d'un champ électrique et d'un champ magnétique. *J. Phys.* (Paris) **3**, 393 (1894).
11. P. Debye. Bemerkung zu einigen neuen Versuchen über einen magneto-elektrischen Richteffekt. *Z. Phys.* **36**, 300 (1926).
12. K.Y. Bliokh, Y.S. Kivshar, and F. Nori. Magnetoelectric effects in local light-matter interactions. *Phys. Rev. Lett.* **113**, 033601 (2014).
13. A.A. Fisher, E.F.C. Dreyer, A. Chakrabarty, and S.C. Rand. Optical magnetization, Part I: Experiments on radiant magnetization in solids. *Opt. Express* **24**, 26064 (2016).
14. A.A. Fisher, E.F.C. Dreyer, A. Chakrabarty, and S.C. Rand. Optical Magnetization, Part II: Theory of induced optical magnetism. *Opt. Express* **24**, 26055 (2016).
15. J. Bucaro and T. Litovitz. Rayleigh scattering: collisional motions in liquids. *J. Chem. Phys.* **54**, 3846 (1971).

16. J. McTague and G. Birnbaum. Collision-induced light scattering in gaseous Ar and Kr. *Phys. Rev. Lett.* **21**, 661 (1968).
17. L. Frommhold. Collision-induced scattering of light and the diatom polarizability. *Adv. Chem. Phys.* **46**, 1, (1981).
18. J. Stevens, G. Patterson, P. Carroll, and G. Alms. The central Lorentzian in the depolarized Rayleigh spectra of CCl_4 and $GeCl_4$. *J. Chem. Phys*. **76**, 5203 (1982).
19. S. Shapiro and H. Broida. Light scattering from fluctuations in orientations of CS_2 in liquids. *Phys. Rev.* **154**, 129 (1967).
20. P. Madden. The depolarized Rayleigh scattering from fluids of spherical molecules. *Mol. Phys.* **36**, 365 (1978).
21. P.J. Chappell, M.P. Allen, R.I. Hallem, and D. Kivelson. Theory of depolarized light scattering. *J. Chem. Phys.* **74**, 5929 (1981).
22. S.C. Rand, W.M. Fisher, and S.L. Oliveira. Optically-induced magnetization in homogeneous dielectric media. *J. Opt. Soc. Am. B* **25**, 1106 (2008).
23. A.A. Fisher, E.F.C. Cloos, W.M. Fisher, and S.C. Rand, "Dynamic symmetry-breaking in a simple quantum model of magneto-electric rectification, optical magnetization, and harmonic generation", *Opt. Express* **22**, 2911 (2014).
24. E.F.C. Dreyer, A.A. Fisher, P. Anisimov, and S.C. Rand, "Optical magnetism, Part III: Theory of molecular magneto-electric rectification", Optics Express (under review).
25. W. Phadungsukanan, S. Shekar, R. Shirley, M. Sander, R.H. West, M. Kraft. First principles thermochemistry for silicon species in the decomposition of tetraethoxysilane. *J. Phys. Chem. A* **113**, 9041 (2009).
26. T. Shinoda. Qualitative classification of tetrahedral molecular crystals. *Mol. Cryst. Liquid Cryst*. **76**, 191 (1981).
27. Y.R. Shen. *The Principles of Nonlinear Optics*. pp. 286-296 (J. Wiley & Sons, New York, 1984)
28. T. Shimanouchi. *Tables of Molecular Vibration Frequencies.* Vol. 1 in NSRDS-NBS, National Bureau of Standards (1972).
29. I. Ignatyev, A. Lazarev, T. Tenisheva, B. Shchegolev. Molecular structure, force field and vibrational spectra of tetra methoxysilane. *J. Mol. Struct.* **244**, 193 (1991).
30. M. Van der Vis, R. Konings, A. Oskam, and T. Snoeck. The vibrational spectra of gaseous and liquid tetraethoxysilane. *J. Mol. Struct.* **274**, 47 (1992).
31. G. Herzberg. *Spectra of Diatomic Molecules.* Second edition, P. 68, (Van Nostrand Reinhold Co., Toronto, 1950)
32. A. Briguet, J. Duplan, and J. Delmau. Molecular reorientation of liquid silicon tetrachloride. *Mol. Phys.* **39**, 1541 (1980).
33. G. Causley and B. Russell. The vacuum ultraviolet absorption spectra of the group Iva tetrachlorides. *J. Electron Spectrosc. Relat. Phenom.* **11**, 383 (1977).

Acknowledgements
This research was supported by the MURI Center for Dynamic Magneto-optics, the Air Force Office of Scientific Research (FA9550-12-1-0119 and FA9550-14-1-0040), and a DURIP grant (FA9550-15-1-0307). The authors thank H. Winful for useful discussions.

Author Contributions

S.C.R. conceived the project with contributions from M.T.T., and E.F.C.D. M.T.T. designed and carried out the experiments and data analysis, with input from K.M. Samples were prepared by K.M., A.S., S.J.Y. and J.K. Computer-control of data acquisition was provided by E.F.C.D. All the authors took part in regular discussions and contributed to the writing of the manuscript.

Competing Interests
The authors declare no competing financial interests

Additional Information
Supplementary information is available for this paper
Reprints and permission information is available at www.nature.com/reprints
Correspondence and requests for materials should be addressed to T.M.T.

Publisher's note: Springer Nature remains neutral with regard to jurisdictional claims in published maps and institutional affiliations.

Methods

Light source and scattering experiments

The light source for our scattering experiments was a regeneratively amplified mode-locked Ti:sapphire laser that delivered 0.5 mJ pulses with central photon energy of 1.55 eV at a repetition rate of 10 kHz. The pulse bandwidth was electronically variable between 15-100 nm. The incident collimated beam passed through a polarization rotator that was computer-controlled and was directed without focusing into liquid samples prepared in sealed quartz cuvettes inside a light tight box. Light scattered at 90^{o} was collected and collimated by a lens with an effective numerical aperture of 0.002. The spectrum of scattered light was measured with a resolution of 0.01 nm by replacing the photomultiplier with a 0.5 m Andor spectrometer fitted with a CCD camera in the output plane. See Supplementary Information for more detail.

Sample Preparation

The anhydrous chemicals used in this research were spectroscopic grade, purchased from Sigma Aldrich Inc., and were examined in quartz cuvettes with very high quality surfaces after rinsing with DI water, acetone, and isopropanol in a sequence and transferring them immediately to an oven, where they were heated at a temperature > 82 C for ~ 20 minutes. Cleaning and sealing of the cuvettes was performed inside a glovebox to prevent hydration of the samples. Just before each measurement, the four outer surfaces of the sample cuvette were given a final cleaning with optical tissue paper wetted with MeOH and blown dry using pressurized nitrogen gas.

Data analysis.

See Supplementary Information.

Data availability. The data that support the plots within this paper and other findings of this study are available from the corresponding author upon request.